

- Title: **Numerical Simulation of Temperature Gradients for the Mass Concrete Foundation Slab of Shanghai Tower**
- Authors: Jian Gong, Shanghai Construction Group  
Weijiu Cui, College of Civil Engineering, Tongji University  
Yong Yuan, College of Civil Engineering, Tongji University  
Xiaoping Wu, Shanghai Construction Group
- Subject: Geotechnic/Foundation
- Keywords: Concrete  
Foundation
- Publication Date: 2015
- Original Publication: International Journal of High-Rise Buildings Volume 4 Number 4
- Paper Type:
1. Book chapter/Part chapter
  2. **Journal paper**
  3. Conference proceeding
  4. Unpublished conference paper
  5. Magazine article
  6. Unpublished

# Numerical Simulation of Temperature Gradients for the Mass Concrete Foundation Slab of Shanghai Tower

Jian Gong<sup>1,2,†</sup>, Weijiu Cui<sup>1</sup>, Yong Yuan<sup>1</sup>, and Xiaoping Wu<sup>2</sup>

<sup>1</sup>College of Civil Engineering, Tongji University, Shanghai 200092, China

<sup>2</sup>Shanghai Construction Group Co., Ltd., Shanghai 200080, China

---

## Abstract

Crack control remains a primary concern for mass concrete structures, where the majority of cracking is caused by temperature changes during the hydration process. One-time pouring is a useful construction method for mass concrete structures. The suitability of this method for constructing on of the Shanghai Tower's mass concrete foundation slab of Shanghai Tower is considered here by a numerical simulation method based on a 6-meter-thick slab. Some of the conclusions, which can be verified by monitoring results conducted during construction, are as follows. The temperature gradient is greater in the vertical direction than in the radial direction, therefore, the vertical temperature gradient should be carefully considered for the purpose of crack control. Moreover, owing to cooling conditions at the surfaces and the cement mortar content of the slab, the temperatures and temperature gradients with respect to time vary according to the position within the slab.

**Keywords:** Shanghai Tower, Mass concrete, Numerical simulation, Temperature gradient

---

## 1. Introduction

Concrete foundation slab and huge-columns of super high-rise buildings are mass concrete components. Prevention of early cracking in these components remains a key issue during construction of super high-rise building. The main causes of early cracking involve thermal issues and shrinkage, where, for mass concrete structures, thermal issues are more significant. Because the concrete pouring volume of foundation slabs is typically much larger than that of huge-columns, the early cracking of foundation slabs caused by thermal issues is more obvious. To address this problem, the maximum concrete pouring volume per time is limited by many building codes worldwide. For example, many construction codes for mass concrete allow for three possible construction methods: setting deformation seam, post pouring belt construction and alternative bay construction. Concrete structures formed by these methods naturally have seams at the junction, this can cause stress concentration and leakage issues.

Temperature and related issues are core concerns for crack control in foundation slabs, and they have been studied by numerous researchers. Yuan and Wang (2002) proposed an analytical model to predict thermal expansion in young concrete under various conditions as a means of evaluating the potential for cracking, making the model

useful as a reference for planning the construction of mass concrete structures. As is known, the main heat source of mass concrete derives from cement hydration. Chu et al. (2013) provided a method for predicting hydration-induced thermal stress precisely, which is employed for establishing the most appropriate construction method and cracking controlling temperature. Another method for inhibiting early cracking is to reduce hydration by adding fly ash or slag. Wang and Lee (2010) conducted a simulation of the hydration of concrete containing fly ash or slag, where the heat evolution rate was determined according to the contributions from both cement hydration and the reaction of the mineral admixtures. The incorporation of cooling water pipes has also been employed for decreasing the temperature of mass concrete. Liu et al. (2015) established through simulation and monitoring of a mass concrete dam that the temperature of the concrete was reduced nearby the cooling pipes. All the above researches has been shown to be useful for control of early cracking, and these methods can be employed for one-time concrete pouring of mass concrete (its benefits can be known from the first paragraph).

With the rapid development of computer technology, three-dimensional (3D) analysis has been widely used to investigate the thermal issues of mass concrete. The present study builds upon this development to investigate the temperature gradients within a mass concrete slab foundation. Firstly, the basic concepts involved with temperature gradients are discussed for the later analysis. A 3D numerical model is then established, and the numerical

---

<sup>†</sup>Corresponding author: Jian Gong

Tel: +; Fax: +

E-mail: cuiweijiu@163.com

simulation of a mass concrete foundation slab is conducted using Abaqus. Meanwhile, some important viewpoints are given including the validity of one-time pouring for mass concrete. Finally, the numerical stimulation results are compared with field monitoring data.

### 2. Theoretical Model of the Hydration Heat of Mass Concrete

Hydration heat is the primary cause of the temperature rise observed in mass concrete, and the hydration heat is usually large in mass concrete structure. If the developing heat can-not be sufficiently released, the temperature of the concrete in the core area becomes extremely high, while the temperature of the concrete at the surface of the concrete is relatively low. This condition creates a large temperature gradient that makes early cracking more prone to occur.

The rate at which the hydration heat is released is therefore one of the key influencing factors of early cracking, where the heat release rate is related to the thermal conductivity of the material. We therefore employ the heat conduction equation given as Eq.(1). For mass concrete, the equation is comprised of two parts, where the first part is the temperature gradient ( $\nabla_i \cdot \theta$ ) and the second part is the hydration heat release( $\dot{Q}$ ). Therefore, both parts are essential for stimulating the thermal issues of mass concrete. The following sections provide a detailed introduction to the stimulation work.

$$\frac{\partial T}{\partial t} = \alpha \left( \frac{\partial^2 T}{\partial x^2} + \frac{\partial^2 T}{\partial y^2} + \frac{\partial^2 T}{\partial z^2} \right) + \frac{\partial \theta}{\partial t} \tag{1}$$

### 3. General Review of Foundation Pit Slab of the Shanghai Tower

The shape of the foundation pit slab of Shanghai Tower is symmetrical, and its top surface is a circular while its bottom surface is octagonal in shape. The majority of the foundation pit is 6.1 m thick except that in pit in pit is 12 m, the geometrical dimensions of the slab are illustrated in Fig. 1.

The foundation slab’s total pouring amount is 61,200 m<sup>3</sup> (this includes 1,200 m<sup>3</sup> of the pit in pit) represented a world record. The strength grade of the concrete was C50 and its anti-permeability level was P12. To meet the construction need, a one-time mass concrete pouring method was adopted for this project. As discussed in Section2, the hydration heat produced by the mass concrete structure was extremely large. Therefore, a numerical simulation was conducted to establish whether or not this method was theoretically feasible.

### 4. Numerical Simulation of Mass Concrete

Numerical stimulation is an effective method in engineering research, and the establishment of an appropriate is of vital importance. This section introduces the 3D model employed in the present study, based on the mass concrete foundation slab of Shanghai Tower.

#### 4.1. The finite model

Based on model symmetry, a finite element model of a 1/4 section of the foundation slab shown in Fig. 2 is employed in Abaqus to reduce the calculational burden. The adopted 3D solid element types and model size are listed in Table 1. Because the simulation is conducted only for

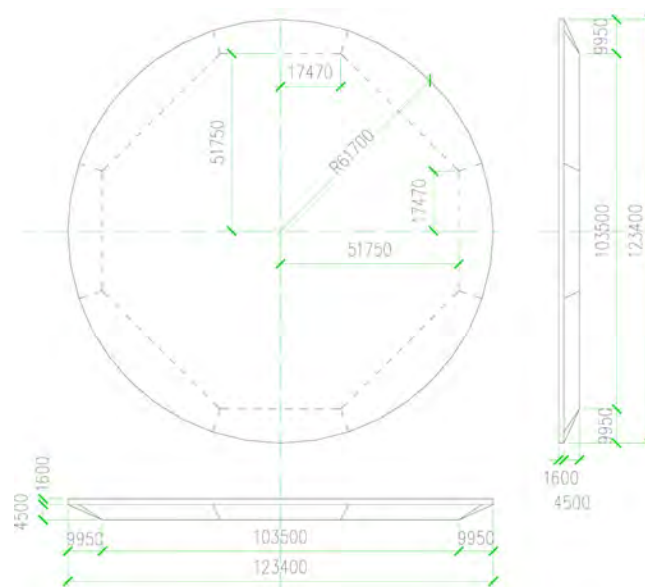
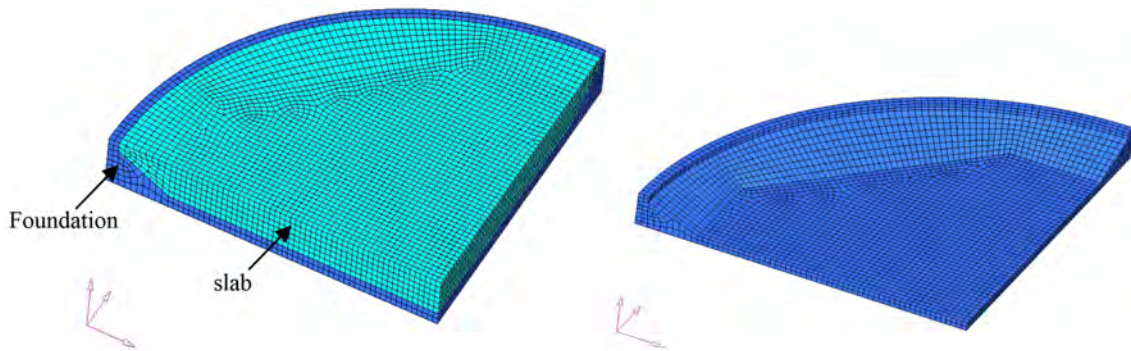


Figure 1. The geometrical dimensions of the foundation pit slab of Shanghai Tower.



**Figure 2.** The overall finite element model (left) and the concrete foundation model (right).

**Table 1.** The scale of the overall finite element model

	soil	concrete	total
Element type	DC3D8	DC3D8	/
Number of the element	15576	31148	46724
Number of nodes	11366	18857	30223

**Table 2.** Material characteristics

/	concrete	soil
Unit weight $\gamma$ (kN/m <sup>3</sup> )	24.0	18.0
Thermal conductivity $\lambda$ (kJ/(m·h·°C))	10.0	3.0
Specific heat (kJ/(kg·°C))	0.96	1.05

temperature, each node of the 8 node DC3D8 solid element only contains the temperature freedom degrees. To considering the influence of the soil around and under the concrete slab on heat conduction, a layer of soil about 2m thick soil was established around and under the bottom of the concrete slab. Heat loss was considered at the lateral side, bottom side, and top surface. The material characteristics appropriate to standard engineering practice for the soil and concrete employed in the model are listed in Table 2.

The surface convection coefficient of concrete has a substantial effect on its surface temperature, the value of this coefficient is usually determined according to different insulation measures. When a template or a heat insulating layer is considered on the concrete surface, the additional layer is calculated as a third boundary condition,

although the heat release coefficient is determined such as consider the effect of the template or insulating layer.

$$\beta_s = \frac{1}{(1/\beta) + \sum(h_i/\lambda_i)} \quad (2)$$

Here the  $\beta_s$  is the heat transfer coefficient of the outermost insulation layer in the air;  $h_i$  is the thickness of the insulation layer;  $\lambda_i$  is the thermal conductivity of the insulation layer.

The top surface convection is modeled as follows. When the surface is exposed, it is considered as a rough surface with a wind speed of 2 m/s, and the equivalent heat release coefficient is 53 kJ/(m<sup>2</sup>·h·°C). When the surface is covered with two layers of thin film and two layers of straw bags, the equivalent heat release coefficient is 8 kJ/(m<sup>2</sup>·h·°C). When the surface is covered with a single layer of film, and a single layer of straw bags, the equivalent heat release coefficient is 14 kJ/(m<sup>2</sup>·h·°C); In the present calculation, the heat transfer coefficient for the top surface of the concrete is selected as 8 kJ/(m<sup>2</sup>·h·°C) (i.e., condition9(b)).

Ignoring of the effect of temperature differences between day and night, we applied a constant ambient temperature of 15°C; and the casting temperature of the concrete was assumed to be 20°C. The boundary conditions of the model are listed in Table 3.

#### 4.2. The arrangement of data collection points

To evaluate the temperature change, nodes along the C axis and S axis are taken as the temperature-time data col-

**Table 3.** Boundary conditions of the model

adiabatic temperature rise (°C)	47.24
initial temperature of concrete (°C)	20.0
initial temperature of soil (°C)	15.0
environment temperature (°C)	15.0
top surface convection coefficient of concrete (kJ/(m <sup>2</sup> ·h·°C))	8.0
side surface convection coefficient of soil (kJ/(m <sup>2</sup> ·h·°C))	2.0
bottom surface convection coefficient of soil (kJ/(m <sup>2</sup> ·h·°C))	1.0
top surface convection coefficient of soil (kJ/(m <sup>2</sup> ·h·°C))	5.0
symmetric plane of the model	Symmetric boundary

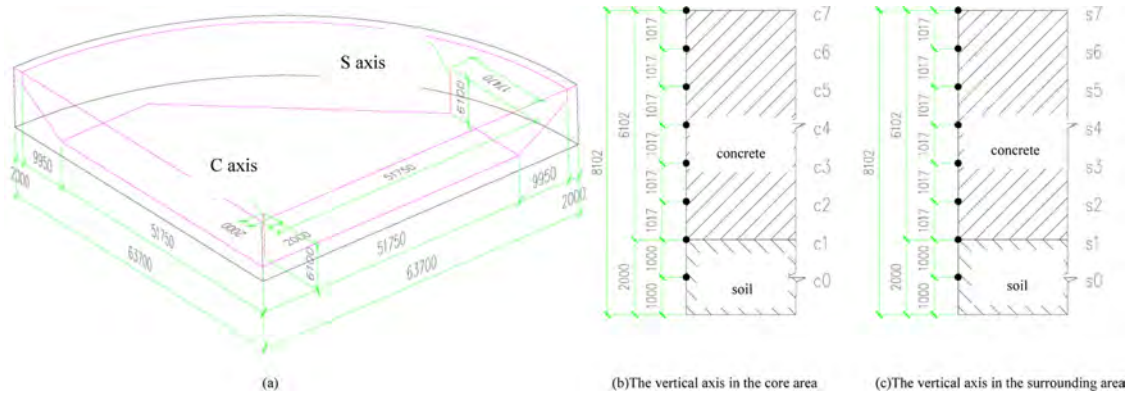


Figure 3. Temperature time collection points and their indices along the C and S axes.

lection points, where, as shown in Fig. 3(a), the C axis is a vertical axis in the core area that is 2 m away from both symmetrical faces, and the S axis is a vertical axis in the surrounding area that crosses the top point of the octagonal bottom of the foundation slab. The distance between nodes and indices are shown in Figs. 3(b) and 3(c).

### 5. Discussion and Analysis

#### 5.1. Analysis of temperature

##### 5.1.1. The temperature-time analysis

The temperature versus time curves of points C<sub>j</sub> and points S<sub>j</sub> (j = 1, 2, 3, 4, 5, 6) given in Fig. 3 are shown in Fig. 4. From Fig. 4 we see that the temperature trends of the collection points are in accord with the temperature change law of mass concrete. The observed trend can be divided into three stages: rapid heating stage, slow cooling stage and temperature stabilization stage.

##### (a) Rapid heating stage

After concrete pouring, the cement hydration released a large quantity of heat, and the temperature increased rapidly, and reaching a maximum value on about the 3rd day.

##### (b) Slow cooling stage

The temperature begins to decrease slowly as the rate of heat release begins to exceed the rate of heat production with gradually reduced hydration. This stage usually continues for an extended period.

##### (c) Temperature stabilization stage

The temperature stabilizes, and the final temperature resides close to the ambient temperature.

Although the temperature-time curves are similar, some differences are observed between the core area (C axis) and the surrounding area (S axis).

(a) The maximum temperature value was higher in the core area, where the highest temperature was about 58.2°C Fig. 4 (left).

(b) The temperature decreased more slowly in core area, where the rate of decrease was about 0.3 °C/d, which meets the standard requirement that the cooling rate should be less than 2°C/d in the standard.

The main reason for the above conditions was that the concrete in the surrounding area had a more favorable cooling condition, which facilitated the release of the hydration heat; therefore, its rate of temperature decrease

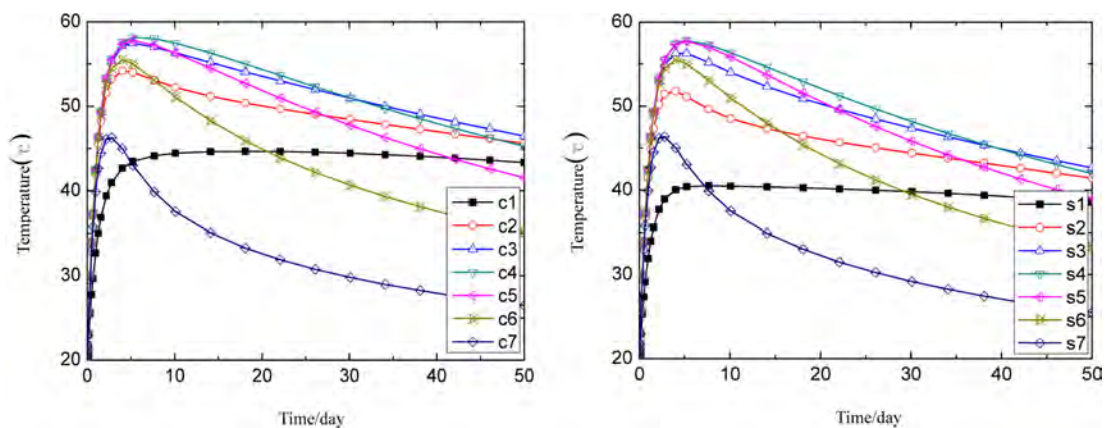


Figure 4. The temperature versus time curves of the collection points (left - C axis, right - S axis).

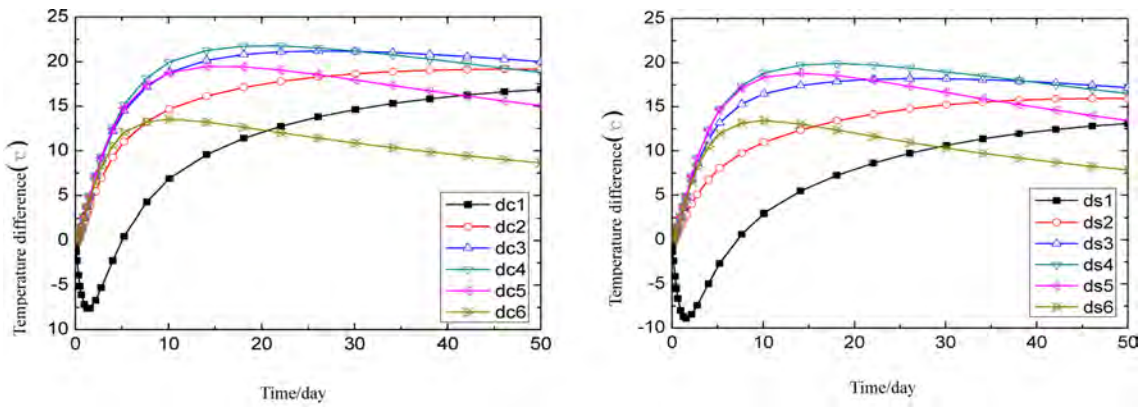


Figure 5. The temperature difference versus time curves of the collection points (left - C axis, right - S axis).

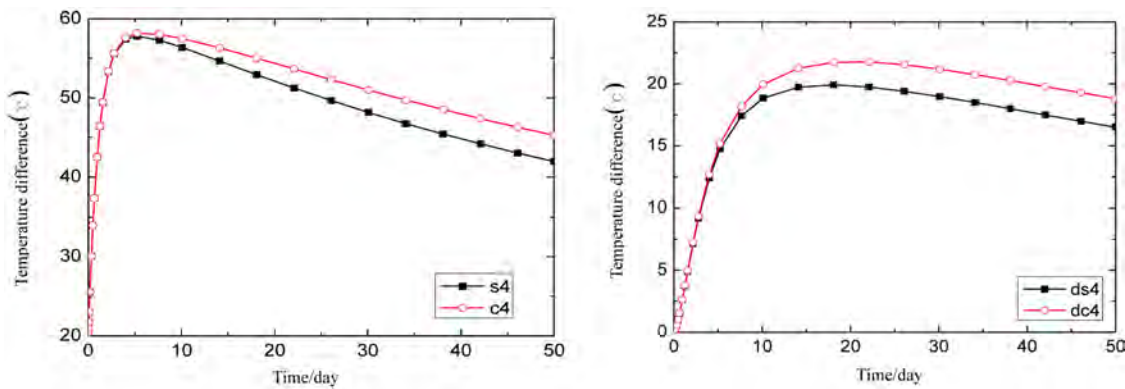


Figure 6. The core temperature of the middle region ( $j=4$ ) and the temperature difference between the middle and the top surface.

speed was greater, while heat released more slowly in the core area, and maintained a relatively higher temperature.

5.1.2. The temperature difference-time analysis

The temperature difference versus time curves of collection points along the C and S axes are shown in Fig. 5, where  $dc_j$  represents  $C_j$ - $C_7$  and  $ds_j$  represents  $S_j$ - $S_7$  ( $j=1, 2, 3, 4, 5, 6$ ). The maximum temperature difference between the middle region ( $j=4$ ) and the top surface ( $j=7$ ) along the C and S axes were  $21.8^{\circ}\text{C}$  and  $19.9^{\circ}\text{C}$  respectively. The temperature versus time in the middle region of the two axes are compared in Fig. 6 (left), and a comparison of their maximum temperature differences between inside and outside were shown in Fig. 6 (left). The reason for the observed differences is that the concrete hydration heat around the S axis is more likely to be released owing to proximity to the surface relative to conditions around the C axis.

5.1.3. The soil temperature-time analysis

Consideration of the boundary condition was vitally important in the simulation, such that the soil under the

foundation slab was also considered. The temperature versus time curves of the soil 1-m from the bottom of foundation slab (i.e., for  $j=0$ ) are shown in Fig. 7. The temperatures versus time curves were unlike those obtained for the mass concrete slab. Because the mass concrete foundation slab continuously released its hydration

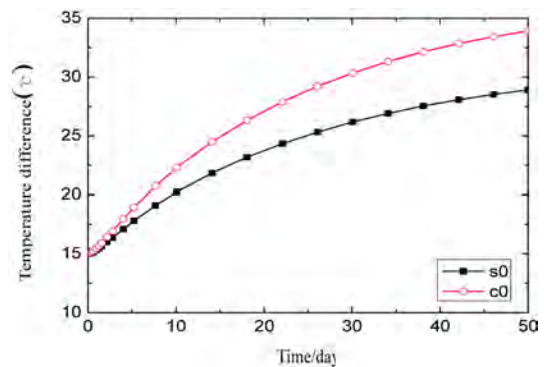


Figure 7. The temperature versus time curves of the soil 1-m from the bottom of the foundation slab ( $j=0$ ).

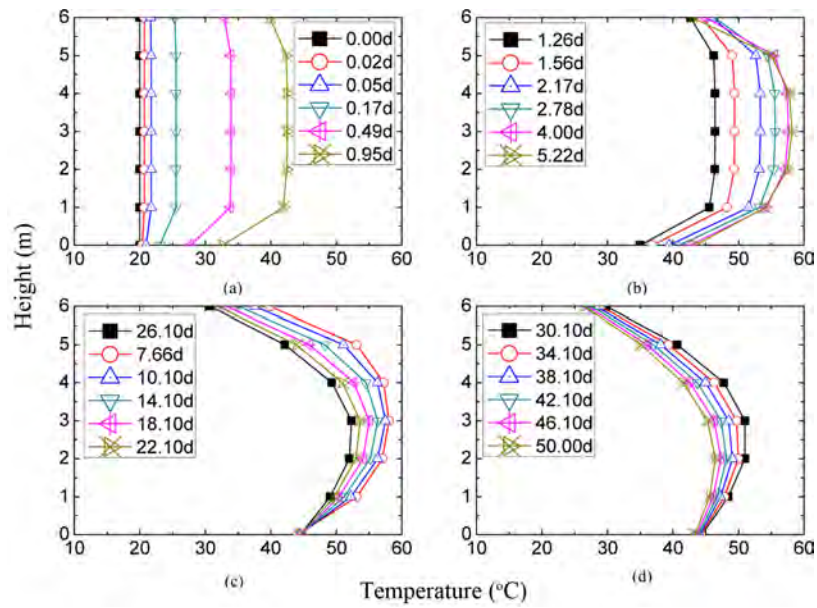


Figure 8. The temperature gradients along the C axis at different moments in time.

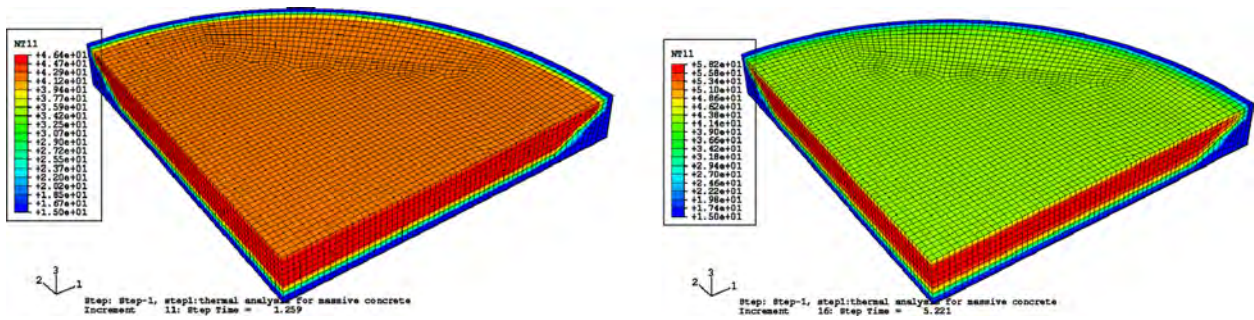


Figure 9. The temperature field distribution after 1.26-d (left) and after 5.22-d (right) (unit: °C).

heat outward, the temperatures of the soil continued to rise, and the total temperature increment was nearly 20°C at the core.

5.1.4. The temperature gradient

The temperature gradients of the core data collection points along the vertical axis at different moments in time are shown in Fig. 8. We can see that, during the 0-d~5.22-d period, the temperature gradient along the axis increased gradually with the release of hydration heat, and the temperature attained its peak value in the core area; After 5.22-d, the temperature gradient along the vertical axis reduced gradually.

5.2. Comparative analysis of the temperature distribution

The temperature field distributions of the concrete at 1.26-d and 5.22-d after pouring are shown in Fig. 9. The temperature distribution indicates that the temperature of

the middle region is greatest, and it gradually decreases from the middle both upward and downward along the vertical direction. Moreover, the temperature near the top surface is greater than that at the bottom surface. Along the radial direction, the temperature distribution remains nearly unchanged.

To analyze the temperature distribution both in the radial direction and in vertical direction, temperature distributions derived from various temperature sections of the model are investigated, and the following section provides a detailed comparison analysis.

5.2.1. Temperature comparison in the radial direction

The temperature distribution of a radial component of the model 2-m away from the symmetric plane obtained 5.22-d after pouring is shown in Fig. 10. The figure presents a number of closed isothermal lines that essentially run parallel with the radial contour of the foundation slab and become more concentrated at the edge of the mass

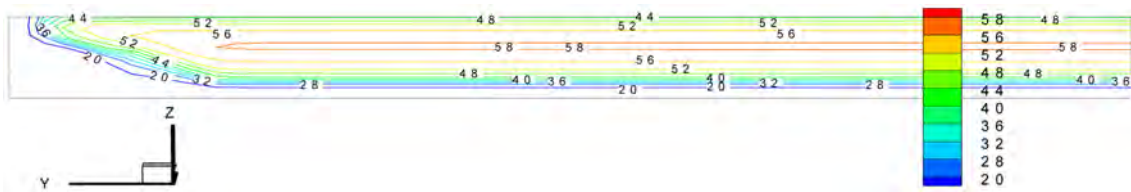


Figure 10. The temperature distribution of a radial section 2-m away from the symmetric plane at 5.22-d (unit: °C).

concrete slab. Clearly, the temperature gradient along the radial direction is small. This indicates that, in a limited height (minor deformation layer), the thermal deformation along the radial direction is approximately equality, although adjacent deformation layers may have different thermal deformations. If the thermal deformation difference surpasses a limiting value, the thermal stress is large enough to cause cracking in mass concrete.

5.2.2. Temperature comparisons in the vertical direction

The temperature distribution in the vertical direction of the mass concrete slab is also important, where the temperature gradient is a key feature. The temperature in middle region is higher at 58°C than the temperature at the contact surface between concrete and soil; moreover, the temperature gradients is larger at the contact surface as well, where the temperature changes by about 28°C over a distance of about 3-m indicating a temperature gradient of about 9.3°C/m. The temperature distributions of different sections of the model are shown in Fig. 11 5.22 d after pouring. As the figure shows, the temperature distributions of the different sections are nearly equivalent, but the temperature of the outer edge of the mass concrete slab is relatively low, because its thickness is less than that of the main body.

Based on a comparison of the different temperature-time curves along a given axis in Fig. 4, it is concluded that, along a given vertical axis, the temperature of the core area is highest, and the temperature near the top surface is greater than that near the bottom surface. At a point closer to the surface, its peak temperature appears

earlier and the subsequent decrease in temperature is more rapid. The main reason for this is the cooling condition prevalent near the surface and the cement mortar content at different heights along the vertical axis. Regarding the cooling condition, the foregoing analysis provides a detailed discussion. Because of the favorable cooling condition, the temperature along the vertical direction is low at both ends. Concrete is a mixture of cement mortar, sand, gravel and water, and, owing to the action of gravity, the heavier components such as gravel are more prone to move downward. Therefore, a great concentration of cement mortar is found in the upper half of the slab, resulting in a greater degree of cement, and a higher temperature than that near the bottom half of the slab.

6. Conclusion

The one time pouring construction method is a new challenge for mass concrete structures. A detailed numerical simulation for the mass concrete foundation slab of Shanghai Tower was conducted, and the results were compared with the monitoring ones. Some conclusions are as follows,

- a. The one time pouring construction method is appropriate for use in the construction of mass concrete foundation slabs, and numerical analysis is also a useful method for directing mass concrete construction.
- b. The temperature gradient is a key factor in the crack control of mass concrete foundation slab, where an excessive temperature gradient can cause differences in thermal deformation that can result in thermal

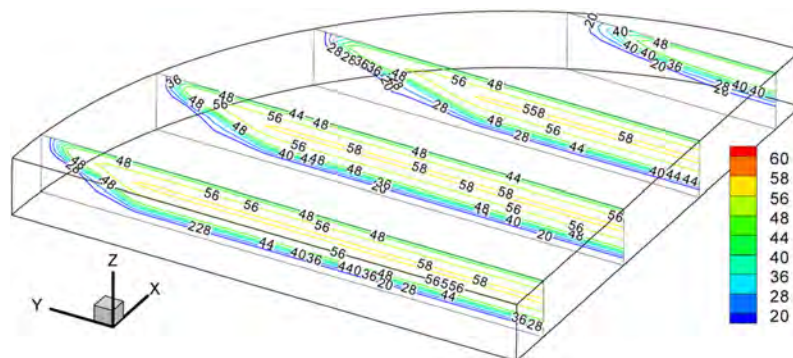


Figure 11. The temperature distribution of different sections 5.22 d after pouring (unit: °C).



stress induced cracking.

- c. Because of the cooling condition near the interface with the surrounding area, the temperature is higher in the core area than that in the surrounding area. Because of the cooling conditions at the bottom and top surfaces of the slab and the cement mortar content, the temperature along a given vertical is higher in the middle region, and the temperature near the top surface is greater than that near the bottom surface. The concrete temperature increases rapidly near the surface reaches its peak early, but the temperature remains at its peak value for only a short period owing to rapid cooling, while the temperature of the core area grows slowly, and the peak value lasts for an extended period owing to its slow cooling rate.
- d. The temperature gradient is larger in the vertical (thickness) direction than that in the radial direction, and, the larger temperature gradient, the more likely the cracking is to occur. Therefore, useful measures should be taken for controlling the temperature gradient in the vertical direction.

## Acknowledgements

This research was supported by the twelfth five year science and technology support program funded by the Ministry of Chinese Science and Technology (Grant No. 2014BAJ03B00).

## References

- Chu, I., Lee, Y., Amin, M. N., Jang, B. S., and Kim, J. K. (2013). "Application of a thermal stress device for the prediction of stresses due to hydration heat in mass concrete structure." *Construction and Building Materials*, 45, pp. 1645~1651.
- Kyle, A. R. (2014). "Statistical determination of cracking probability for mass concrete." *J. Mater. Civ. Eng.* 26, pp. 1~13.
- Liu, X. H, Zhang, C., Chang, X. L, and Zhou, W. (2015). "Precise simulation analysis of the thermal field in mass concrete with a pipe water cooling system." *Applied Thermal Engineering*, 78, pp. 449~459.
- Wang, X. Y. and Lee, H. S. (2010). "Modeling the hydration of concrete incorporating fly ash or slag." *Cement and Concrete Research*, 40, pp. 984~996.
- Yuan, Y. and Wan, Z. L. (2002). "Prediction of cracking within early-age concrete due to thermal drying and creep behavior." *Cement and Concrete Research*, 32, pp. 1053~1059.